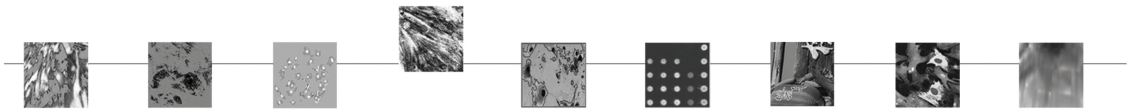

## Chapter 4

# Nitric oxide regulates integrin stimulation-induced hypertrophy in neonatal rat cardiomyocytes



Jim Swildens, Antoine A.F. de Vries, Zhongyan Li, Conrad Schreuders, Douwe E. Atsma, Martin J. Schalij, Ernst E. van der Wall, Arnoud van der Laarse

## Abstract

**Introduction** Our research group previously showed that integrin stimulation with a RGD motif-containing pentapeptide (GRGDS) causes hypertrophy of neonatal rat cardiomyocytes (NRCMs).[1] **Purpose of the study** To investigate the effects of varying the NO-delivering capacity of NRCMs on GRGDS-induced hypertrophy. **Methods** NO production in NRCMs was either inhibited by treatment with the NO synthase (NOS) inhibitor L-NAME or by transduction with lentivirus vectors (LVs) encoding PIN (protein inhibitor of neuronal NOS [NOS1]) or a *NOS1*-specific short hairpin RNA (shNOS1) or was stimulated by incubation with the NO donor sodium nitroprusside (SNP) or with lipopolysaccharide (LPS), which triggers synthesis of inducible NOS (NOS2). The NRCMs were stained for nuclei and $\alpha$-actinin to quantify cell surface area (CSA). Intracellular levels of PIN, shNOS1, NOS2, AKT1/2 (AKT), phospho-AKT1/2/3 (P-AKT) and phospho-S6 kinase were determined directly of indirectly by (immuno)fluorescence microscopy and/or western blotting. **Results** GRGDS-induced hypertrophy of NRCMs was dose-dependently blocked by L-NAME, which blockade could be overcome by SNP treatment. Suppression of NOS1 activity or production of PIN or shNOS1 inhibited GRGDS-induced hypertrophy, dependent on the expression level of the transgene. When either SNP or 8-Br-cGMP were administered together with GRGDS to *PIN*-transduced NRCMs, hypertrophy was rescued. Integrin stimulation-induced hypertrophy was associated with a 3- to 4-fold increase in P-AKT/AKT ratio, which increase was antagonized by L-NAME. Pharmacological inhibitors of soluble guanylate cyclase, phosphatidylinositol 3-kinase and AKT1/2/3 suppressed the GRGDS-induced increase in mean CSA as did the forced expression of a dominant-negative version of AKT1. AKT overexpression led to NRCM hypertrophy that was partly antagonized by rapamycin. LPS treatment without integrin stimulation also caused an increase in the average CSA of NRCMs, dependent on intracellular NOS2 level. LPS-induced NRCM hypertrophy was prevented by L-NAME. **Conclusion** NO is involved in the regulation of integrin stimulation-dependent hypertrophy of NRCMs and exerts at least part of its hypertrophic effects through activation of the PI3K/AKT signaling pathway.

## 4.1 Introduction

The contractile activity of cardiomyocytes leads to their periodic shortening and lengthening, but at the same time these cells experience the movements of neighboring cardiomyocytes. These movements are sensed by various mechanosensors in the sarcolemma including stretch-activated ion channels and integrins.[2] Integrins are heterodimeric transmembrane protein complexes directly linking the extracellular matrix (ECM) to the cytoskeleton.[3,4] Binding of integrins by ECM components or ECM-like substances leads to cellular signaling involving, amongst others, p130 Crk-associated substrate (p130 CAS) family members, focal adhesion kinase (FAK), Src family kinases, Crk, the integrin-linked kinase (ILK)-PINCH-parvin complex, Nck[5-9] and possibly neuronal NO synthase (nNOS/NOS1). [1,10] Using neonatal rat cardiomyocyte (NRCM) cultures, our research group previously showed that integrin ligation by a pentapeptide (GRGDS) containing the Arg-Gly-Asp (RGD) sequence resulted in (**i**) elevated intracellular Ca2+ and NO concentrations[10] and (**ii**) intracellular Ca2+ and NO concentration-dependent cellular hypertrophy.[1]

In the present study, we examined whether integrin stimulation-induced hypertrophy of NRCMs could be modulated by changing the bioavailability of NO via (**i**) overexpression of a recombinant gene encoding the protein inhibitor of NOS1 of rats (PIN), (**ii**) short hairpin RNA (shRNA)-mediated inhibition of rat *NOS1* expression, (**iii**) lipopolysaccharide (LPS)-induced inducible NOS (iNOS/NOS2) production,[11] (**iv**) incubation with $N^G$-nitro-L-arginine methyl ester (L-NAME) which is a general inhibitor of all NOS isoforms including endothelial NOS (eNOS/NOS3) and (**v**) exogenous NO supplementation by the NO donor sodium nitroprusside (SNP). PIN, also called dynein light chain LC-8-type I, is a 89-amino-acid protein that inhibits NOS1 activity by destabilizing its dimeric structure.[12]

The recombinant *PIN* gene and the expression unit specifying the rat *NOS1*-specific shRNA (shNOS1) were introduced in the NRCMs using self-inactivating human immunodeficiency type 1 vectors (SIN-LVs) that also contained a *green fluorescent protein* (GFP) gene for quantifying transduction levels.

NO exerts its biological effects primarily via the intracellular NO receptor soluble guanylate cyclase (sGC), whose catalytic activity is enhanced by binding of NO leading to an increase in cGMP production and subsequent signaling via protein kinase G.[13] We hence investigated the role of active sGC in GRGDS-induced NRCM hypertrophy by using a specific inhibitor of sGC, 1*H*-[1,2,4]oxadiazolo-[4,3-*a*]quinoxalin-1-one (ODQ)[14] and a cell-permeable cGMP analogue, 8-Br-cGMP, to bypass the ODQ-imposed block of sGC activity.

Finally, to address the issue of whether integrin stimulation of cardiomyocytes leads to physiological or pathological hypertrophy,[15-19] we studied the role of phosphoinositide-3-kinase (PI3K)/AKT signaling in the GRGDS-induced changes of NRCM surface area. To this end, we employed the PI3K inhibitor wortmannin, AKT-specific and phospho (P)-AKT-specific antibodies, the isoform-nonselective AKT inhibitor SH-6, the mammalian target of rapamycin (mTOR) inhibitor rapamycin and LVs encoding either a dominant-negative version of murine AKT1 (DN-AKT1) or a constitutively active AKT1. Our results support a model in which integrin stimulation of NRCMs leads to NO-dependent phosphorylation of AKT and consequently a P-AKT-dependent physiological hypertrophic response.

## 4.2 Materials and methods

### 4.2.1 Cardiomyocyte cultures

Cultures of ventricular cardiomyocytes of two-day-old rats were prepared as described before.[20] Briefly, ventricular myocardium was dissociated with collagenase (CLS-2; Worthington, Lakewood, NJ, USA) and the resulting cell suspension was transferred to plastic dishes (Falcon Primaria; BD Biosciences, Breda, the Netherlands) to allow preferential attachment of non-cardiomyocytes. One h later, non-adherent cells were transferred to Petri dishes (Falcon Primaria; ∅35 mm), each containing a glass coverslip (∅25 mm) coated with rat tail collagen type I solution (20 $\mu$g/mL; Sigma-Aldrich, Zwijndrecht, the Netherlands). The culture medium consisted of Ham's F10 medium supplemented with 10% heat-inactivated fetal bovine serum (FBS), 10% heat-inactivated horse serum (HS), 100 U/mL penicillin and 100 $\mu$g/mL streptomycin (all from Invitrogen, Breda, the Netherlands). The culture medium was replaced 24 h after seeding of the cells by a 1:1 ($^{v}/_{v}$) mixture of HamâĂŹs F10 medium and Dulbecco's modification of Eagle's medium (DMEM; Invitrogen) containing 5% HS, antibiotics and 100 $\mu$mol/L 5-bromo-2-deoxyuridine (BrdU; Sigma-Aldrich) to inhibit proliferation of cardiac fibroblasts. The NRCM cultures were kept in a humidified incubator at 37 °C and 5% $CO_2$. The medium was replaced 24 h after the start of the BrdU treatment by a 1:1 ($^{v}/_{v}$) mixture of Ham's F10 medium and DMEM containing 2.5% HS and antibiotics. The experiments had the approval of the Animal Experiments Committee of the Leiden University Medical Center (LUMC).



### 4.2.2 Construction of SIN-LV shuttle plasmids

The coding sequence of the rat *PIN* gene was amplified from IMAGE clone 6887897 (imaGenes, Berlin, Germany) by polymerase chain reaction (PCR) in a total volume of 50 $\mu$L using 50 ng template, 0.5$\mu$mol/L of forward (5'-CAGACGCGTATGTGCGACCGGAAGG-3') and 0.5 $\mu$mol/L of reverse (5'- CCACTCGAGTTAACCAGATTTGAACAGGA-3') primer, 200 $\mu$mol/L of each dNTP, 1× Phusion HF buffer (Finnzymes, Espoo, Finland) and 1 U Phusion High-Fidelity DNA polymerase (Finnzymes). The PCR was performed according to the protocol provided with the DNA polymerase using an annealing temperature of 60°C and 35 amplification cycles. The 288-bp PCR product was purified from a 1% agarose gel using the JETSORB Gel Extraction Kit (GENOMED, Löhne, Germany), digested with MluI and XhoI and combined with the 8.4-kb MluI×XhoI fragment of pLV.CMV.IRES.eGFP[21] using T4 DNA ligase (Fermentas, St. Leon-Rot, Germany). The resulting SIN-LV shuttle plasmid pLV.CMV.rPIN.IRES.eGFP and the starting construct pLV.CMV.IRES.eGFP (negative control) were used for generating SIN-LV particles as described below.

To repress rat *NOS1* expression, a SIN-LV shuttle construct encoding a shRNA targeting the mouse *NOS1* gene and matching perfectly with the coding sequence of the rat *NOS1* gene was obtained from the MISSION shRNA library (Sigma-Aldrich; clone TRCN0000072123). As negative control, another SIN-LV shuttle plasmid from the MISSION shRNA library (clone TRCN0000045425) encoding a shRNA targeting the human *NOS1* gene (CONsh) was used. The 5' end of this shRNA has 3 mismatches with the

rat *NOS1* gene and should therefore have no effect on *NOS1* expression in NRCMs. In both constructs, the puromycin N-acetyl transferase-coding sequence was replaced by that of the GFP of *Renilla reniformis* (hrGFPI) to allow easy assessment of transduction efficiencies. To this end, plasmid pLV.hPGK.hrGFPI (nucleotide sequence available upon request) was digested with SpeI and KpnI and the resulting 1.1-kb DNA fragment containing the hrGFPI-coding sequence was combined with the 6.2-kb SpeI×KpnI fragment of the two SIN-LV shuttle constructs from the Mission shRNA library using T4 DNA ligase.

To investigate the role of Akt1 signaling in the hypertrophic response to GRGDS stimulation, we constructed the SIN-LV shuttle plasmid pLV.CMV.iCA-AKT1.IRES.eGFP (nucleotide sequence available upon request) encoding the *Aequorea victoria* enhanced green fluorescent protein (eGFP) and a constitutively active version of human AKT1 (iCA-AKT1) whose activity is induced by 4-hydroxytamoxifen (4-OHT). The iCA-AKT1 protein was rendered constitutively active by adding the first 14 amino acids of the chicken Src protein, which encompass a myristoylation consensus sequence, to the N-terminus of human AKT1.[22] In addition, the ligand-binding domain of mouse estrogen receptor 1 was fused to the C-terminus of human AKT1, causing it to bind to heat shock protein 90 (Hsp90) in the absence of 4-OHT. In the presence of 4-OHT, iCA-AKT1 is released from Hsp90 enabling it to mediate downstream signaling.



To block AKT signaling, a plasmid encoding a dominant-negative version of mouse AKT1 designated DN-AKT1 was obtained from Addgene (plasmid 16243).[23] This plasmid was digested with SmaI and HincII and the 1.4-kb fragment containing the DN-AKT1-coding sequence was combined with the 8.2-kb SmaI fragment of pLV.CMV.IRES.eGFP using T4 DNA ligase to generate pLV.CMV.DN-AKT1.IRES.eGFP.

All restriction enzymes were from Fermentas. Ligation mixtures were introduced in chemocompetent GeneHogs cells (Invitrogen) and large stocks of the correct plasmids were prepared with the aid of the JETSTAR 2.0 Plasmid Maxiprep Kit (GENOMED).

### 4.2.3 SIN-LV production

Vesicular stomatitis virus G protein-pseudotyped SIN-LVs were produced in 293T cells as described previously.[21] The gene transfer activity of the vector stocks was determined by end-point titration on HeLa indicator cells using flow cytometric analysis of *eGFP* (LV.CMV.IRES.eGFP, LV.CMV.rPIN.IRES.eGFP, LV.CMV.iCA-AKT1.IRES.eGFP and LV.CMV.DN-AKT1.IRES.eGFP) or *hrGFPI* (shRNA-encoding SIN-LVs) expression as read-out. The titers of the SIN-LV preparations are thus expressed in HeLa cell-transducing units (HTUs) per mL.

Forty-eight to 72 h after seeding, the NRCMs were transduced with SIN-LV particles at a vector dose of 5 HTUs/cell in case of the eGFP-encoding SIN-LVs and of 10 HTUs/cell for the shRNA-specifiying SIN-LVs (*i.e.* LV.shNOS1.PGK.hrGFPI and LV.CONsh.PGK.hrGFPI). The next day, the NRCMs were washed three times with phosphate-buffered saline (PBS) and subsequently provided with fresh culture medium. At 7 days post-transduction, the cultures were used for further experiments.

### 4.2.4 Experimental protocol

Integrin stimulation of NRCM cultures was accomplished by adding the pentapeptide GRGDS (Sigma-Aldrich; 10 mg/mL in PBS) to the culture medium to reach a final concentration of 300 $\mu$g/mL. Cells that received PBS (30 $\mu$L/mL of culture medium) only served as negative control. To pharmacologically inhibit NOS activity, we used L-NAME (Sigma-Aldrich; 10 mmol/L stock solution in PBS) at final concentrations of 5, 10, 20 or 100 $\mu$mol/L. Exogenous NO was generated by adding SNP (pharmacy of LUMC; 20 mg/mL stock solution in PBS) to the culture medium at final concentrations of 5, 10, 20 or 40 $\mu$g/mL. L-NAME was added 30 min prior to GRGDS addition and SNP was added just prior to GRGDS addition. To induce NOS2 activity, NRCMs were incubated with 10$\mu$g/mL LPS (Sigma-Aldrich; 10 mg/mL stock solution in PBS) for 48 h. At 24 h after the addition of LPS to the culture medium, the NRCMs were treated with 100 $\mu$mol/L L-NAME or an equivalent volume of vehicle for another 24 h. Earlier, it has been demonstrated that NOS2 is detectable in cultured NRCMs already 6 h after exposure to 10 $\mu$g/mL LPS.[11]



### 4.2.5 (Immuno)fluorescence microscopy

Twenty-four h after GRGDS addition, the NRCMs were rinsed 3 times with PBS + 1$\%$ FBS (PBSF), fixed by a 30-min incubation in 4$\%$ buffered formaldehyde (Klinipath, Duiven, the Netherlands), washed twice with PBSF and permeabilized by incubation for 30 min in PBS + 0.1$\%$ Triton X-100 (Sigma-Aldrich). After washing twice with PBSF, the cells were incubated overnight at 4°C with mouse monoclonal anti-sarcomeric $\alpha$-actinin antibody (A7811; Sigma-Aldrich) diluted 1:400 in PBSF and, in a separate series of experiments, with rabbit anti-NOS2 antibodies (ab3523; Abcam, Cambridge Science Park, Cambridge, UK) at 1:400 dilution. After washing twice with PBSF, the cells were incubated with 500$\times$ diluted secondary antibodies for 60 min. Rabbit anti-mouse IgG conjugated to AlexaFluor 568 (A11061; Invitrogen) was used for labeling the anti-$\alpha$-actinin antibody and the anti-NOS2 antibodies were visualized using donkey anti-rabbit IgG conjugated to AlexaFluor 488 (A21206; Invitrogen). Following two wash steps with PBSF, the cultures were stained with Hoechst 33342 (Invitrogen; 10 $\mu$g/mL in PBSF) for 8 min. After washing twice with PBSF, the coverslips were mounted on microscope slides using Vectashield (Vector Laboratories, Burlingame, CA, USA). Immunofluorescence images were produced using a fluorescence microscope (Nikon Eclipse; Nikon Europe, Badhoevedorp, the Netherlands) equipped with a digital camera (Nikon DXM 1200). As a measure of cell hypertrophy, NRCM surface area (CSA) was determined since average CSA has been proven to correlate well with other measures of NRCM hypertrophy, like [$^3$H]-leucine incorporation.[24] CSA was quantified by morphometric analysis of $\alpha$-actinin-stained NRCMs using Image Pro Plus software (Media Cybernetics, Silver Spring, MD, USA). Typically, per experimental group the CSA of $\geq$5 randomly picked NRCMs per field were determined in multiple fields.

### 4.2.6 Assessment of the relationship between PIN level and NRCM hypertrophy

Of randomly selected LV.CMV.rPIN.IRES.eGFP-transduced NRCMs from 5 independent experiments we determined, with the aid of Image Pro Plus, the eGFP signal intensity and CSA as indirect and direct measures of PIN concentration and GRGDS-induced hypertrophy, respectively. Signal intensity of eGFP ranged from 0 to 70 arbitrary units (AUs) per cell. For several eGFP/PIN signal thresholds, the average CSA of all cells with an eGFP signal ≥N AUs and the mean CSA of all cells with an eGFP signal intensity <20 AUs were calculated. The percentage inhibition of hypertrophy in the different subpopulations of cells displaying relatively higher eGFP signals and thus containing relatively more PIN was calculated for several signal thresholds N between 20 and 70 AUs using the formula: 100 - {[mean % GRGDS-induced hypertrophy (eGFP threshold ≥N) / mean % GRGDS-induced hypertrophy (eGFP threshold <20)] × 100}.

### 4.2.7 Investigation of the relationship between shNOS1 level and NRCM hypertrophy



Of 40-50 NRCMs per coverslip we determined, with the aid of Image Pro Plus software, the hrGFPI signal intensity as an indirect measure of shNOS1 concentration and the CSA as a measure of hypertrophy. Signal intensity of hrGFPI ranged from 0 to 250 AUs per cell.

### 4.2.8 Assessment of the relationship between NOS2 level and NRCM hypertrophy

Of at least 50 NRCMs per coverslip CSA and NOS2 content were determined by analysis of immunofluoromicrographs using Image Pro Plus software. Signal intensity of NOS2 ranged from 25 to 55 AUs per cell.

### 4.2.9 Investigation of the role of sGC in GRGDS-induced NRCM hypertrophy

The major intracellular NO receptor is the enzyme sGC, which after binding of NO to its heme moiety increases it catalytic activity up to 400-fold.[25,26] We used 1*H*-[1,2,4]oxadiazolo-[4,3-*a*]quinoxalin-1-one (ODQ; Sigma-Aldrich; 10 $\mu$mol/L) to selectively inhibit sGC[14] and 8-Br-cGMP (Sigma-Aldrich; 0.5 mmol/L) to circumvent the blockade of sGC by ODQ.

### 4.2.10 Investigation of the role of Src family kinases (SFKs) in the transduction of integrin stimulation-dependent prohypertrophic signals

Since Src family kinases (SFKs) are important mediators of integrin stimulation-dependent cell signaling,[9,27] we used the SFK inhibitor 4-amino-1-*tert*-butyl-3-(1'-naphthyl)pyra-

zolo [3,4-d]pyrimidine (PP1 analogue; 30 $\mu$mol/L; Merck Chemicals, Darmstadt, Germany) to test the importance of this non-receptor tyrosine kinase for GRGDS-induced NRCM hypertrophy.

### 4.2.11 Study of the involvement of PI3K in the transduction of integrin stimulation-dependent prohypertrophic signals

To investigate whether PI3K is implicated in GRGDS-induced NRCM hypertrophy, we analyzed the effect of various concentrations of the PI3K inhibitor wortmannin (10, 50, 100, 500 and 1000 nmol/L; Sigma-Aldrich; 1 mmol/L stock solution in PBS) on the average CSA of GRGDS-treated NRCMs. NRCMs not exposed to GRGDS were treated in parallel with the same range of wortmannin doses to distinguish between the effects of the PI3K inhibitor on integrin ligation-independent and on integrin stimulation-induced CSA. After 24 h of incubation, the average CSA of the NRCMs in the two cultures was $x_n$ and ($x_n$+$y_n$), respectively, with n representing one of the 5 wortmannin doses. Two parallel cultures of NRCMs were incubated without wortmannin, one without GRGDS and one with GRGDS. After 24 h of incubation the mean CSA of the cardiomyocytes in the two cultures was X and (X+Y), respectively. The average CSA in the control culture without GRGDS and without wortmannin was set to 100% with the inhibitory effect of a particular dose of wortmannin on integrin ligation-independent CSA being equal to (X-$x_n$). The inhibiting effect of a specific dose of wortmannin on GRGDS-induced CSA is equal to (Y-$y_n$).

### 4.2.12 Study of the involvement of AKT in the transduction of integrin stimulation-dependent prohypertrophic signals

In NRCMs that had been incubated for 24 h without or with GRGDS (300 $\mu$g/mL) in the absence or presence of 100 $\mu$mol/L of L-NAME, AKT and P-AKT levels were quantified by immunocytology using 1:500 dilutions of goat anti-human-AKT1/2 (sc-1619; Santa Cruz Biotechnology, Santa Cruz, CA, USA) and of rabbit anti-human-P-AKT1/2/3 (sc-7985-R; Santa Cruz Biotechnology) antibodies, respectively. The latter antibodies recognize an epitope including the phospho-serine residue in the AKT regulatory domain ($Ser^{437}$ for human AKT1). The primary antibodies were detected by AlexaFluor 568-conjugated donkey anti-goat IgG (A11057; Invitrogen) and AlexaFluor 488-conjugated donkey anti-rabbit IgG, respectively, both at 1:500 dilution.

In a separate series of experiments, we prepared cell homogenates by scraping $\approx 6 \times 10^5$ cells in 0.5 mL ice-cold lysis buffer, after 24 h of incubation without or with GRGDS (300 $\mu$g/mL). Lysis buffer consisted of 50 mmol/L Tris-HCl (pH 8.0), 150 mmol/L NaCl, 1% Nonidet P-40 (Merck Chemicals), 1 mmol/L sodium orthovanadate (Sigma-Aldrich) + freshly added protease inhibitors (Protease Inhibitor Cocktail Tablets; Roche, Almere, the Netherlands). Cell homogenates were stored at -80°C until use in western blot analysis. To this end, proteins were separated in a NuPage 10% Bis-Tris gel (Invitrogen) with MOPS as running buffer, and electro-transferred onto a polyvinylidene fluoride membrane (Hybond-P, GE Healthcare Europe, Diegem, Belgium), which was processed essentially as described before.[1] As a molecular weight marker Full Range

Rainbow marker (RPN800E; GE-Healthcare Europe) was used. AKT1/2 and P-AKT1/2/3 were labeled with the same antibodies as used for their immunocytological detection. The anti-AKT1/2 and anti-P-AKT1/2/3 antibodies were used at dilutions of 1;10,000 and 1:100,000, respectively. As secondary antibodies we employed donkey anti-goat IgG conjugated to horseradish peroxidase (HRP; sc-2020, Santa Cruz Biotechnology] at a dilution of 1:20,000 and goat anti-rabbit IgG-HRP (sc-3837; Santa Cruz Biotechnology) at a dilution of 1:50,000. Glyceraldehyde 3-phosphate dehydrogenase (GAPDH) was used for normalization purposes. This housekeeping protein was detected using a mouse monoclonal anti-GAPDH antibody (MAB374; Millipore, Billerica, MA, USA) at a dilution of 1:100,000 and 100,000× diluted goat anti-mouse IgG-HRP (sc-2005; Santa Cruz Biotechnology). Chemiluminescence was induced with the aid of an ECL Advance Western Blotting Detection Kit (GE Healthcare Europe) and signal intensities were determined with the aid of the ChemiDoc XRS+ Imager (Bio-Rad Laboratories, Veenendaal, the Netherlands).

To test whether ribosomal protein S6 kinase (S6K) is part of the signaling pathway involved in integrin stimulation-induced cardiomyocyte hypertrophy and to corroborate that S6K acts downstream of AKT, NRCMs were incubated with and without GRGDS in the absence and presence of the AKT inhibitor SH-6 (20 $\mu$mol/L; ENZO Life Sciences, Zandhoven, Belgium). Next, P-S6K levels were determined by immunocytology using rabbit anti-P-S6K antibodies (S6311; Sigma-Aldrich) at 1:250 dilution in combination with 500× diluted AlexaFluor 488-conjugated donkey anti-rabbit IgG.



Besides by using the phosphatidylinositol analogue SH-6, AKT inhibition was also accomplished by transducing NRCMs with a SIN-LV encoding DN-AKT1 and eGFP. In DN-AKT1 the lysine residue at position 179 is substituted by a methionine, resulting in a version of AKT1 that lacks kinase activity.[23] NRCMs transduced with LV.CMV.IRES.eGFP instead of LV.CMV.DN-AKT1.IRES.eGFP served as negative control in this experiment.

Mice overexpressing constitutively active AKT1 proteins demonstrated an increase of myocardial mass.[24,28-30] To test the effects of constitutive high-level AKT signaling on cardiomyocyte hypertrophy, NRCMs were transduced with a bicistronic SIN-LV encoding iCA-AKT1 and eGFP. In the absence of 4-OHT, iCA-AKT1 is maintained in an inactive state through association with Hsp90. Incubation of the cells with 250 nmol/L 4-OHT (Sigma-Aldrich) causes disruption of the iCA-AKT1-Hsp90 complex leading to the activation of iCA-AKT1.

### 4.2.13 Statistics

Results are expressed as means ± standard error of the mean (SEM), unless stated otherwise. The significance of differences between means was calculated by Student's *t*-test and one-way analysis of variance followed by the Bonferroni's *post hoc* test whenever appropriate using SPSS16 for Windows (SPSS, Chicago, IL, USA). Linear and non-linear fits were calculated in Graph Pad Prism 4 (Graph Pad Software, La Jolla, CA, USA). Experimental results were always compared with data from control experiments performed at the same day. Differences were considered significant if $p<0.05$.

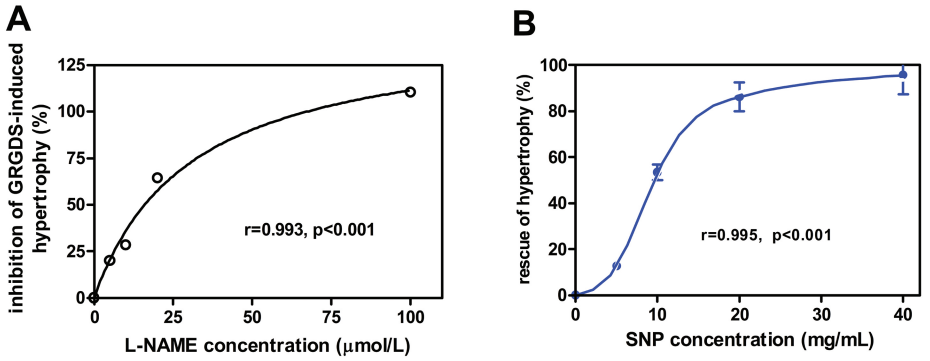


**Figure 4.1: A.** Percentage inhibition of GRGDS-induced NRCM hypertrophy is plotted against the L-NAME concentration. Per data point 51-67 cells were analyzed. **B.** Percentage stimulation of hypertrophy of NRCMs treated with GRGDS (300 $\mu$g/mL) plus L-NAME (100 $\mu$mol/L) by various doses of SNP. Per data point 42-88 cells were analyzed.

4

## 4.3 Results

### 4.3.1 The NOS inhibitor L-NAME represses GRGDS-induced NRCM hypertrophy

Previous work of our research group pointed to the involvement of NO signaling in the integrin stimulation-dependent hypertrophic response of cardiomyocytes.[1,10] Using several concentrations of the NOS inhibitor L-NAME, ranging from 5 to 100 $\mu$mol/L, we found an inhibition of GRGDS-induced NRCM hypertrophy which was dependent on the L-NAME concentration (fig. 1A). By non-linear correlation analysis the correlation coefficient was 0.993 ($p<0.001$).

### 4.3.2 Exogenous NO donor administration can overcome L-NAME-dependent inhibition of GRGDS-induced NRCM hypertrophy

In NRCMs that were stimulated by GRGDS, hypertrophy was inhibited completely by 100 $\mu$mol/L of L-NAME, but if combined with 5 to 40 $\mu$g/mL of the NO donor SNP, inhibition was attenuated. Following treatment with 40 $\mu$g/mL SNP, the average CSA in L-NAME-treated NRCMs went up to 95.6$\pm$8.1% of that of GRGDS-treated NRCMs not exposed to L-NAME or SNP ($r=0.995$; $p<0.001$) (fig. 1B).

### 4.3.3 Inhibition of NOS1 activity by forced PIN expression blocks GRGDS-induced NRCM hypertrophy

The observation that treatment of NRCMs with GRDGS peptides led to an increase in the amount of NOS1 molecules activated by phosphorylation at serine residue 1446[1] sug-

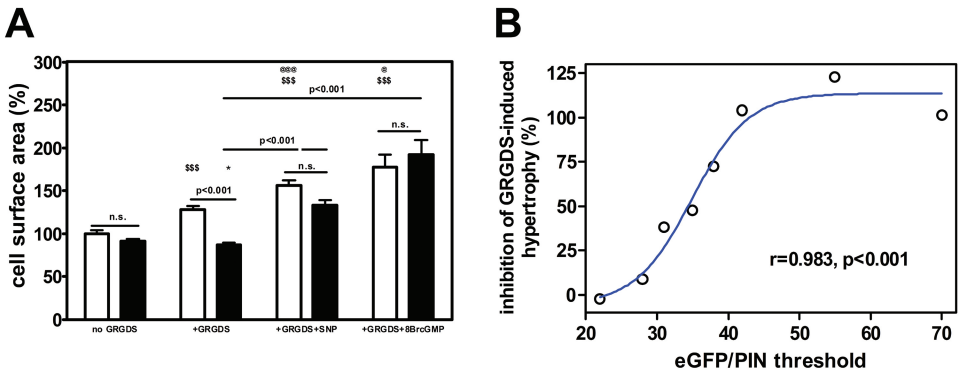


**Figure 4.2: A.** Mean CSAs (±SEM) of NRCMs transduced with LV.CMV.IRES.eGFP (white bars) or with LV.CMV.rPIN.IRES.eGFP (black bars), treated for 24 h without GRGDS, with GRGDS (300 $\mu$g/mL), with the combination of GRGDS (300 $\mu$g/mL) and SNP (10 $\mu$g/mL) and with the combination of GRGDS (300 $\mu$g/mL) and 8-Br-cGMP. All bars are normalized to the average CSA of untransduced NRCMs incubated without GRGDS, SNP and 8-Br-cGMP. Numbers of cells analyzed are, from left to right, 128, 146, 178, 211, 109, 114, 10 and 10, obtained from 5 independent experiments. $$$ p<0.001 vs. "no PIN, no GRGDS"; @ p<0.05 and @@@ p<0.001 vs. "no PIN, +GRGDS". * n.s. vs. "+PIN, no GRGDS". **B.** Percentage inhibition of GRGDS-induced hypertrophy of NRCMs is plotted against the eGFP/PIN threshold value. Per data point, 31-46 cells were analyzed for eGFP intensity.



gested an important role for this NOS isoform in integrin stimulation-dependent cardiomyocyte hypertrophy. To further investigate the contribution of NOS1 to GRGDS-induced cardiomyocyte hypertrophy, NRCMs were transduced with LV.CMV.rPIN.IRES.eGFP, a bicistronic SIN-LV coding for eGFP and the selective NOS1 inhibitor PIN or with the control vector LV.CMV.IRES.eGFP, which only directs the synthesis of eGFP. Averaged over 5 independent experiments, the pro-hypertrophic effect of the RGD motif-containing pentapeptide GRGDS was 28.0±3.8% as determined from the CSAs of 178 NRCMs (fig. 2A). In NRCMs that had been transduced with LV.CMV.rPIN.IRES.eGFP, a nonsignificant decrease in average CSA was observed as compared to control cells both in the absence (-9.1±2.9%) and presence (-13.3±2.2%) of GRGDS. As expected from its site of action, the PIN-imposed block on GRGDS-induced hypertrophy was bypassed by SNP (10 $\mu$g/mL) and by the cell-permeable cGMP analogue 8-Br-cGMP (0.5 mmol/L) resulting in increases in mean CSA of 33.4±6.2%, and of 92.2±17.0%, respectively, in comparison to LV.CMV.IRES.eGFP-transduced NRCMs not exposed to GRGDS (Fig. 2A).

In LV.CMV.rPIN.IRES.eGFP-transduced and GRGDS-treated NRCMs, eGFP signal intensity, an indirect measure of *PIN* expression level, correlated negatively with CSA by non-linear correlation analysis (r=-0.49; n=50; p<0.001). For several eGFP/PIN thresholds (between 22 and 70 AUs as determined by fluorescence microscopy), we determined the mean percentage of GRGDS-induced hypertrophy of all NRCMs above a certain eGFP/PIN threshold and divided that by the mean percentage of GRGDS-induced hypertrophy of all NRCMs below an eGFP/PIN threshold of 20. Non-linear correlation

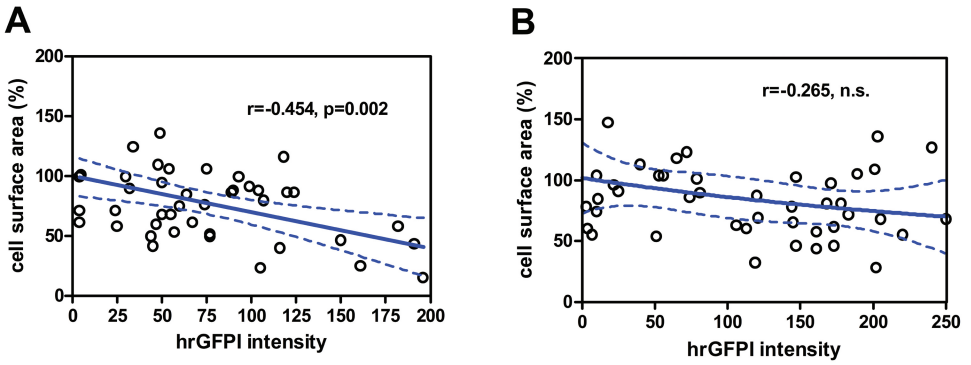


**Figure 4.3: A.** The CSA (AUs) of NRCMs transduced by LV.shNOS1.PGK.hrGFPI is negatively correlated with shNOS1 levels determined by measurement of hrGFPI signal intensity. Number of data points is 43. **B.** The CSA of NRCMs transduced by LV.CONsh.PGK.hrGFPI, which codes for a shRNA targeting a sequence in the human NOS1 transcripts that contains 3 mismatches with the rat NOS1 gene, does not correlate with hrGFPI signal intensity as an indirect measure of CONsh concentration. Number of data points is 45.



analysis (fig. 2B) revealed that the extent of inhibition of GRGDS-induced NRCM hypertrophy by PIN was dependent on its intracellular concentration (r=0.983; p<0.001).

### 4.3.4 Knockdown of NOS1 expression by RNA interference inhibits GRGDS-induced NRCM hypertrophy

To confirm, by an independent method, the involvement of NOS1 in integrin stimulation-induced cardiomyocyte hypertrophy, NRCMs were transduced with a SIN-LV coding for a NOS1-specific shRNA or for a non-targeting control shRNA. In NRCMs that had been infected with LV.shNOS1.PGK.hrGFPI, hrGFPI signal intensity, an indirect measure of shNOS1 level, ranged from 0 to 200 AUs (as determined by fluorescence microscopy). In these cells, CSA after integrin stimulation was inversely correlated with hrGFPI signal intensity (r=-0.454; n=44; p=0.002) (fig. 3A). Conversely, in LV.CONsh.PGK.hrGFPI-transduced NRCMs that were treated with 300 $\mu$g/ml GRGDS, no correlation between CSA and hrGFPI signal intensity was observed (r=-0.265; n=46; p=n.s.) (fig. 3B).

### 4.3.5 Exogenous 8-Br-cGMP administration can overcome the inhibitory effect of suppressing sGC activity on GRGDS-induced NRCM hypertrophy

In NRCMs that were stimulated by GRGDS, hypertrophy was inhibited completely by 10 $\mu$mol/L ODQ, an inhibitor of sGC (fig. 4). However, if 8-Br-cGMP (0.5 mmol/L) was coadministered with ODQ, hypertrophy occurred to an extent normally observed with GRGDS, and was independent of the presence of GRGDS (fig. 4), indicating that the

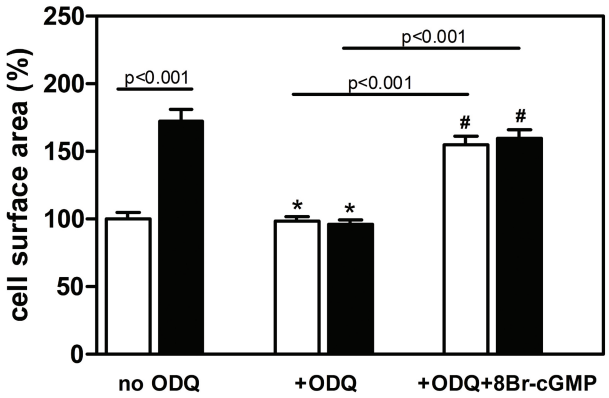


**Figure 4.4:** Mean CSAs (±SEM) of NRCMs treated without GRGDS (white bars) and with GRGDS (300 $\mu$g/mL) (black bars) for 24 h in the absence and presence of ODQ (10 $\mu$mol/L) without or with 8-Br-cGMP (0.5 mmol/L). All bars are normalized to the average CSA of NRCMs incubated without GRGDS, ODQ and 8-Br-cGMP. Numbers of cells analyzed are, from left to right, 23, 23, 22, 18, 19 and 21. * n.s. vs. "no GRGDS, no ODQ". # n.s. vs. "+ GRGDS, no ODQ".

4

NO-responsive system comprising sGC and cGMP is crucial for the integrin stimulation-dependent induction of hypertrophy in NRCMs.

### 4.3.6 Integrin stimulation-induced NRCM hypertrophy does not require SFK activity

Incubation of NRCMs with the specific SFK inhibitor PP1 (30 $\mu$mol/L) influenced neither the cell size of NRCMs incubated in the absence of GRGDS (108.9±18.0% with PP1 versus 100.0±20.0% without PP1; p=n.s.) nor the hypertrophy induced by GRGDS (CSA compared to control cells: 153.8±35.5% with PP1 and 146.9±39.5% without PP1; difference between GRGDS-treated NRCM cultures with and without PP1: n.s.) (mean±standard deviation [SD]).

### 4.3.7 Involvement of PI3K/AKT signaling in integrin stimulation-induced NRCM hypertrophy

While activation of receptor tyrosine kinases and the PI3K/AKT signaling cascade are strongly linked with physiological hypertrophy of cardiomyocytes, G-protein-coupled receptors and the calcineurin/nuclear factor of activated T-cells (NFAT) pathway are key players in pathological cardiac hypertrophy. Investigating the P-AKT/AKT ratio in GRGDS-treated NRCMs and the sensitivity of integrin stimulation-induced hypertrophy in these cells to PI3K inhibition should thus provide information about the nature of the hypertrophic process. Integrin stimulation of NRCMs by GRGDS caused a 3-4 fold increase in P-AKT/AKT ratio, which increase was reduced to <2-fold by the presence of L-NAME (100 $\mu$mol/L) as analyzed by western blotting (fig. 5A). The P-AKT/AKT ratio as deter-

mined by western blotting correlated quite well with that determined by immunocytology (fig. 5B). Thus, integrin stimulation by GRGDS elicits an NO-dependent signaling pathway that includes AKT. Upstream of AKT is PI3K that can be inhibited by wortmannin. Using wortmannin at various concentrations we noticed that the GRGDS-dependent increase in CSA of NRCMs is sensitive to wortmannin at concentrations ≥50 nmol/L (fig. 5D), whereas the GRGDS-independent CSA is not affected by wortmannin treatment (fig. 5C).

AKT activity is inhibited by SH-6 which is a cell permeable, reversible and substrate-competitive phosphatidylinositol analogue that inhibits the activation of AKT. Administration of SH-6 (20 $\mu$mol/L) had no significant effect on the CSA of NRCMs that were incubated without GRGDS for 24 h, but completely inhibited GRGDS-induced hypertrophy of NRCMs (fig. 6A).

AKT activation stimulates phosphorylation (by mTOR complex 1) of the 70-kDa S6K at threonine residue 389.[31] The resulting P-S6K protein stimulates protein synthesis through the phosphorylation of, amongst others, ribosomal protein S6 (rpS6), eukaryotic translation initiation factor 4B and eukaryotic elongation factor-2 kinase. We thus investigated by immunocytology, the effect of integrin stimulation and AKT inhibition on the level of P-S6K in NRCMs. Incubation of NRCMs with GRGDS caused an increase in P-S6K-associated fluorescence of 17.0±4.7% (p=0.005 compared to NRCMs exposed to neither GRGDS nor SH-6) whereas coadministration of SH-6 reduced the P-S6K signal by 34.8±5.6% in comparison to GRGDS-treated cells not incubated with SH-6 (p<0.001) and by 17.8±4.3% compared to NRCMs exposed to neither GRGDS nor SH-6 (p=0.003) (fig. 6B).

Besides through pharmacological interventions, we also studied the involvement of AKT in integrin stimulation-induced cardiomyocyte hypertrophy by genetic means. To this purpose, we employed SIN-LVs encoding either a dominant-negative or constitutively active version of AKT1. Western blot analysis of protein lysates from NRCMs transduced with these SIN-LVs confirmed their functionality with LV.CMV.DN-AKT1.IRES.eGFP directing the synthesis of a 60 kDa protein species indistinguishable from wild-type AKT1 and LV.CMV.iCA-AKT1.IRES.eGFP specifying an AKT1 fusion protein of 105 kDa (fig. 6C).

Consistent with the results of the SH-6 treatment, overexpression of DN-AKT1 did not change the mean CSA of NRCMs incubated without GRGDS, but markedly reduced the GRGDS-induced hypertrophy (from 55.8±8.3% to 27.8±8.4%; p=0.047)(fig. 6D).

Finally, overexpression of iCA-AKT1 induced hypertrophy of NRCMs (by 54.6±8.3%) that was only partially inhibited (to 29.4±8.5%; p=0.052) by 10 nmol/L rapamycin, an inhibitor of especially mTOR complex 1, which is downstream from AKT (fig. 6E).

### 4.3.8 LPS-induced NOS2 activity is equally efficient in promoting NRCM hypertrophy as integrin-stimulation dependent NOS1 activity

To study whether induction of NO signaling by other means than via integrin stimulation or exogenous NO donor administration could also induce cardiomyocyte hypertrophy, NRCMs were exposed to LPS, which triggers NOS2 expression via an NF-$\kappa$B-dependent pathway[32] (fig. 7B-E). Induction of NOS2 resulted in an increase of mean CSA from

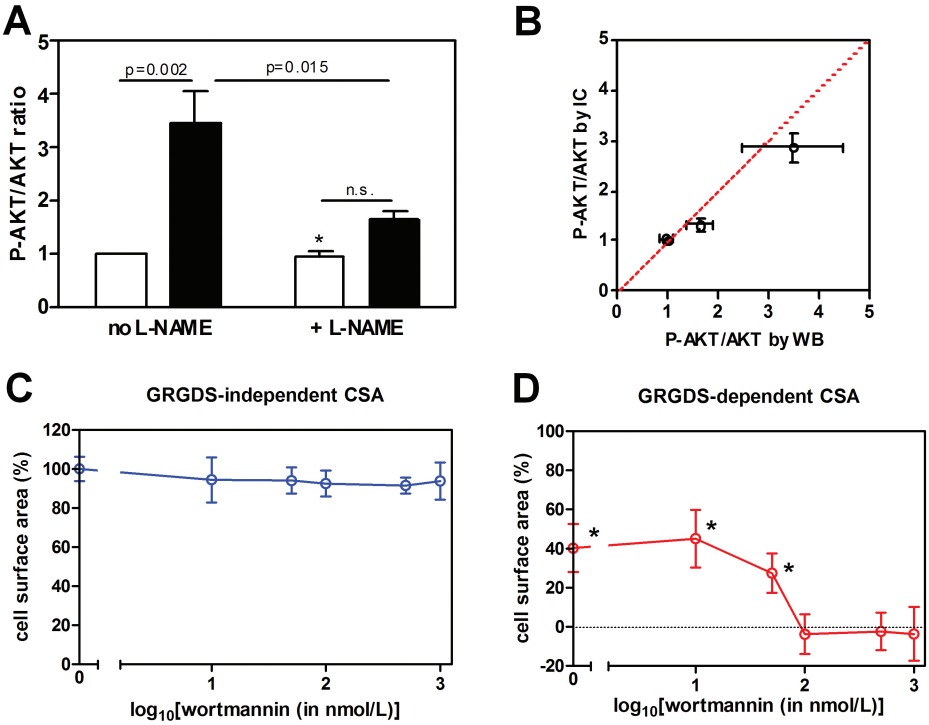


**Figure 4.5: A.** P-AKT/AKT ratio in NRCMs incubated without GRGDS (white bars) or with 300 $\mu$g/mL GRGDS (black bars) in the absence or presence of 100 $\mu$mol/L L-NAME as analyzed by western blotting. All bars are normalized to the average P-AKT/AKT ratio of NRCMs incubated without GRGDS and L-NAME. Numbers of cultures analyzed are, from left to right, 6, 10, 7 and 8. * n.s. vs. "no GRGDS, no L-NAME". **B.** P-AKT/AKT ratios (mean ± SD) were determined by immunocytology (IC; 6-10 cells per data point) and western blotting (WB; 3 cultures per data point) in NRCMs incubated with or without GRGDS (300 $\mu$g/mL) in the absence and presence of 100 $\mu$mol/L L-NAME. The red striped line represents the line of identity. **C.** For wortmannin doses >0 nmol/L, GRGDS-independent NRCM surface area is plotted against the common logarithm of the wortmannin concentration in the culture medium. All CSA values are normalized to the average CSA value of NRCMs incubated without GRGDS and wortmannin. Numbers of cells per data point are 7-14. **D.** For wortmannin doses >0 nmol/L, GRGDS-dependent NRCM surface area is plotted against the common logarithm of the wortmannin concentration in the culture medium. All CSA values are normalized to the average CSA value of NRCMs incubated without GRGDS and wortmannin. Numbers of cells per data point are 7-13. * $p<0.05$ compared to an increase in CSA of 0%.

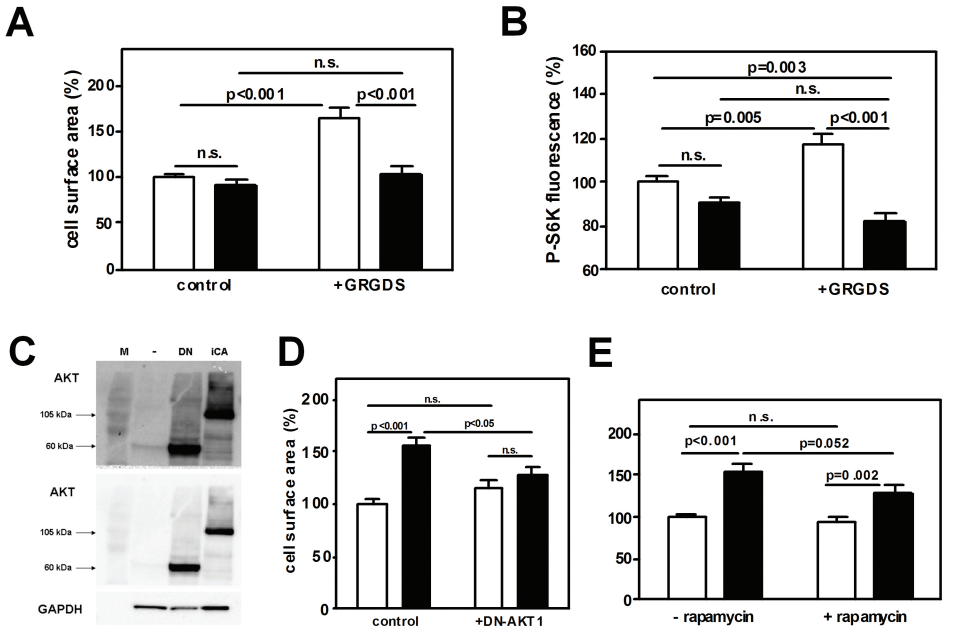


**Figure 4.6: A.** Mean CSAs (±SEM) of NRCMs treated without SH-6 (white bars) and with SH-6 (20 $\mu$mol/L) (black bars) for 24 h in the absence and presence of GRGDS (300 $\mu$g/mL). All bars are normalized to the average CSA of NRCMs incubated without GRGDS and SH-6. Numbers of cells analyzed are, from left to right, 25, 25, 20 and 22. **B.** Mean P-S6K immunofluorescence signal (±SEM) of NRCMs treated without SH-6 (white bars) and with SH-6 (20 $\mu$mol/L) (black bars) for 24 h in the absence and presence of GRGDS (300 $\mu$g/mL). All bars are normalized to the average fluorescence of P-S6K of NRCMs incubated without GRGDS and SH-6. Numbers of cells analyzed are, from left to right, 12, 10, 10 and 10. **C.** Western blot analysis of AKT and GAPDH levels in untransduced NRCMs (-), NRCMs transduced with a SIN-LV encoding DN-AKT1 (DN) and in NRCMs transduced with a SIN-LV encoding iCA-AKT1 (iCA). The two upper panels represent photographs of the same blot at different exposure times. M, molecular weight marker. **D.** Mean CSA (±SEM) of NRCMs transduced with a dominant-negative version of mouse AKT1 (DN-AKT1) or transduced with a LV expressing only the eGFP gene (control) incubated for 24 h in the absence (white bars) and presence (black bars) of GRGDS (300 $\mu$g/mL). Numbers of cells analyzed are, from left to right, 24, 25, 26 and 22. **E.** Mean CSA (±SEM) of NRCMs transduced with LV.CMV.IRES.eGFP (white bars) and of NRCMs transduced with LV.CMV.iCA-AKT1.IRES.eGFP (black bars) treated without and with rapamycin (10 nmol/L). All bars are normalized to the average CSA of NRCMs transduced with LV.CMV.IRES.eGFP not incubated with rapamycin. Numbers of cells analyzed are, from left to right, 29, 23, 25 and 27.

100±29.8% (mean±SD) in the absence of LPS to 125±25.2% after incubation with LPS (10 $\mu$g/mL) for 48 h. The NOS2 concentration in the NRCMs, as quantified by immunocytology, increased from 26.6±7.2 AUs to 42.7±10.7 AUs (p<0.001) by the LPS treatment. The CSA of NOS2-expressing NRCMs positively correlated with NOS2 signal intensity (r=0.48, p<0.005) (fig. 7A). The presence of L-NAME (100 $\mu$mol/L) during the last 24 h of incubation with LPS completely abolished NOS2-dependent NRCM hypertrophy with the consequential loss of the positive correlation between CSA and NOS level (r=-0.08, p=n.s.) (fig. 7A). ODQ (10 $\mu$mol/L) blocked the LPS-induced hypertrophy almost completely; the mean CSA went down to 111.3±31.1% which was not significantly different from NRCMs incubated without LPS and without ODQ. However, coadministration of 8-Br-cGMP (0.5 mmol/L) prevented this ODQ-induced inhibition of LPS-induced hypertrophy, and the average CSA went up to 193.2±35.8% being higher than observed in NRCMs incubated with LPS only (p=0.024)(fig. 7F).

Intense NOS2-specific staining was invariably observed at sites of cell-to-cell contact, implying the association of a fraction of the NOS2 molecules with the sarcolemma (fig. 7G).



## 4.4 Discussion

The present study shows that integrin stimulation of NRCMs leads to hypertrophy via a mechanism involving NO production, sGC activation by NO and cGMP production by activated sGC. This conclusion is based on the finding that complete inhibition of GRGDS-induced NRCM hypertrophy was accomplished using 100 $\mu$mol/L of the general NOS inhibitor L-NAME (fig. 1A) while administration of the NO donor SNP at a dose ≥20$\mu$g/mL to NRCMs pretreated by L-NAME (100 $\mu$mol/L) resulted in almost total (>80%) rescue of integrin stimulation-induced NRCM hypertrophy (fig. 1B). Also, at a dose of 10 $\mu$mol/L the sGC inhibitor ODQ completely blocked the hypertrophic response of NRCMs to GRGDS treatment, which block could be overcome by concurrent incubation of the cells with the cGMP analogue 8-Br-cGMP (fig. 4).

Since previous research has demonstrated that NRCMs express all three NOS genes, [33] each of the three NOS proteins could potentially be involved in the production of NO in response to integrin stimulation. Based on the fact that treatment of NRCMs with GRDGS peptides led to an increase in the amount of NOS1 molecules activated by phosphorylation at serine residue 1446,[1] we focused on the role of NOS1 in integrin stimulation-dependent cardiomyocyte hypertrophy. Accordingly, NRCMs were transduced with a SIN-LV encoding rat PIN. This resulted in a PIN concentration-dependent inhibition of the GRGDS-induced increase in NRCM surface area, which was complete in cells containing high PIN levels (fig. 2B). In the first study on PIN, the protein was shown to interact *in vitro* with NOS1 but not with NOS2 or NOS3 using lysates of 293T cells individually transfected with recombinant versions of each of the NOS genes.[12] Consistently, in lysates of HMC-1 cells, PIN associates with endogenous NOS1 but not with endogenous NOS3.[34] Furthermore, the fact that the PIN-binding site in NOS1 has been located in a region not present in NOS2 or NOS3 makes inhibition of these enzymes by PIN very unlikely.[35] Collectively, these findings implicate NOS1 as the major producer of NO in

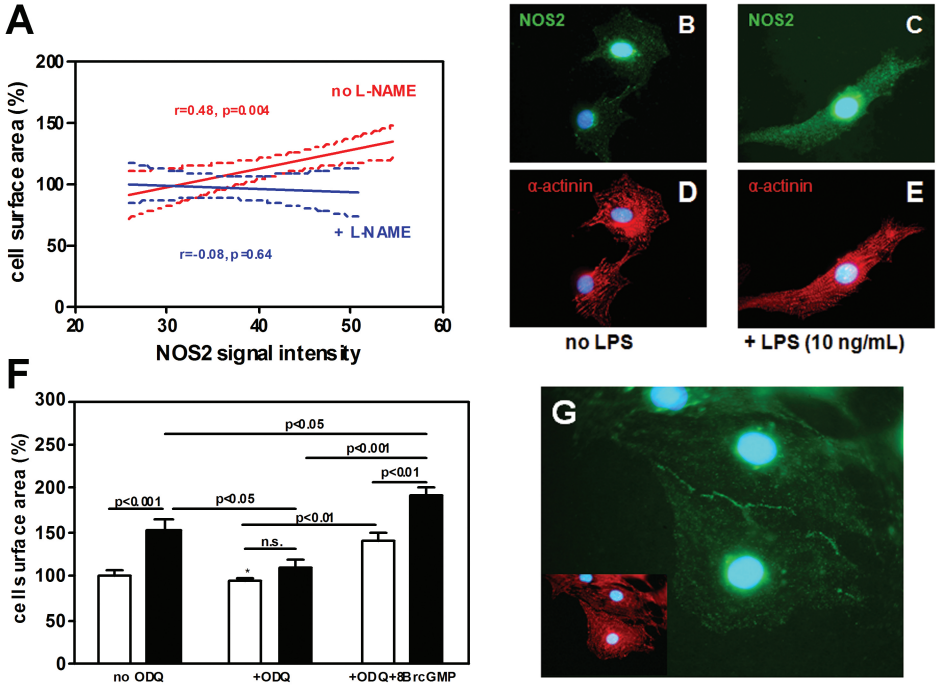


**Figure 4.7: A.** The CSA of NRCMs incubated with LPS (10 ng/mL) to induce NOS2 activity is positively correlated to NOS2 signal intensity (red line and confidence limits, n=33 cells), but in the presence of L-NAME (100 $\mu$mol/L) this correlation is lost (blue line and confidence limits, n=36). All CSA values are normalized to the average CSA value of NRCMs incubated without LPS and without L-NAME. **B-E.** Fluoromicrographs of representative NRCMs showing NOS2 (green fluorescence) and sarcomeric $\alpha$-actinin (red fluorescence) after 48 h of mock treatment (B, D) or after incubation for 48 h with LPS (10 ng/mL) (C, E). **F.** Mean CSAs ($\pm$SEM) of NRCMs treated without LPS (white bars) and with LPS (10 ng/mL) (black bars) for 24 h in the absence and presence of ODQ (10 $\mu$mol/L) without or with 8-Br-cGMP (0.5 mmol/L). All bars are normalized to the average CSA of NRCMs incubated without LPS, ODQ and 8-Br-cGMP. Numbers of cells analyzed are, from left to right, 14, 14, 13, 14, 11 and 14. **G.** Intense NOS2 staining was generally observed at the boundaries of LPS-treated NRCMs demonstrating its clustering underneath the plasma membrane, and particularly at sites adhering to neighboring cells. Insert shows the results of the immunostaining for sarcomeric $\alpha$-actinin, which indicates that both cells are cardiomyocytes.

response to integrin stimulation. The suppressive effect of a shRNA specifically targeting rat *NOS1* transcripts on integrin ligation-dependent NRCM hypertrophy corroborates the key role of NOS1 in GRGDS-induced hypertrophic signaling (fig. 3). However, induction of NOS2 by LPS also resulted in hypertrophic growth of NRCMs which was dependent of NOS2 level. Although LPS will have many other effects on NRCMs, such as induction of contractile dysfunction via Toll-like receptor 4,[36] the observation that 100 $\mu$mol/L L-NAME fully blocked the LPS-induced hypertrophy points to an important role for NOS2-derived NO in stimulating cardiomyocyte growth in response to endotoxin treatment (fig. 7A).

Our results further identified PI3K and AKT as important mediators of integrin stimulation-dependent cardiomyocyte hypertrophy acting downstream of cGMP. However, the observation that treatment of NRCMs with L-NAME at a concentration that fully blocked cardiomyocyte hypertrophy (fig. 1A) did not completely normalize the P-AKT/AKT ratio (fig. 5A), indicates that integrin stimulation of NRCMs results in the phosphorylation of AKT at the serine residue in the regulatory domain not only via an NO-dependent pathway.

The present study did not detect a suppressive role of SFK inhibition by PP1 analogue on hypertrophic growth of NRCMs in response to integrin signaling even though our research group previously showed an increase in phosphorylation of FAK at the tyrosine residue in the SFK docking site ($Y^{397}$ in human FAK) following GRGDS treatment of NRCMs.[10] Consistently, Clemente *et al.* recently found that transgenic mice with cardiomyocyte-specific overexpression of focal adhesion kinase (FAK) displayed concentric cardiac hypertrophy that was associated with enhanced signaling through PI3K, AKT, mTOR, S6K and rpS6, but did not involve the Src/ERK1/2 pathway.[37] Thus, NRCMs should possess an integrin stimulation-dependent but SFK-independent mechanism to activate NOS1.



### 4.4.1 Role of NOS1 in myocardial hypertrophy

NOS1 may exist in different forms as a result of (**i**) alternative RNA splicing, (**ii**) complex formation with itself (dimeric versus monomeric state) or with other proteins such as calmodulin and (**iii**) posttranslational modifications including phosphorylation at various sites.[38-41] In cardiomyocytes, a large fraction of NOS1 colocalizes with ryanodine receptor 2 (RyR2)[42] and regulates the open probability ($P_o$) of this sarcoplasmic reticulum (SR) $Ca^{2+}$ release channel via S-nitrosylation.[43,44] Our research group recently showed that integrin stimulation of NRCMs in culture by an RGD motif-containing peptide is associated with RyR2-dependent intracellular $Ca^{2+}$-release, NO production and hypertrophy.[1,10] On the basis of these findings we proposed an important role for SR-associated NOS1 in integrin stimulation-induced cardiomyocyte hypertrophy. In the present study, we demonstrated that shRNA-mediated inhibition of *NOS1* expression blocked GRGDS-induced hypertrophy of NRCMs in an shRNA dose-dependent manner (fig. 3A). In another study, specific depletion of *NOS1* transcripts by RNA interference was associated with inhibition of phenylephrine-induced (*i.e.* pathological) hypertrophy of NRCMs.[45] In mice overexpressing *NOS1* in cardiomyocytes, aortic constriction caused more left ventricular hypertrophy (LVH) than in wild-type mice that underwent the same treatment.[46] The pressure overload-induced LVH appeared to be of the physiological type as (**i**) myocardial ex-

pression of the genes encoding atrial natriuretic peptide (*NPPA*), brain natriuretic peptide (*NPPB*), Îš-myosin heavy chain (*MYH7*) and $\alpha$-skeletal-actin (*ACTA1*) was barely upregulated, (**ii**) left ventricular remodeling hardly occurred, (**iii**) $Ca^{2+}$ transients were preserved or had increased amplitude and (**iv**) myocardial inotropy and lusitropy had increased, whereas wild-type mice showed pronounced left ventricular dilatation and impaired contractility in response to pressure overload.[46] Adaptive cardiac hypertrophy is not only induced by cardiomyocyte-specific *NOS1* overexpression[46] but also by insulin-like growth factor-1 (IGF1).[47] The signaling pathway activated by IGF1 receptor stimulation[48] resembles the signaling cascade initiated by stretch[49] in many aspects, such as the involvement of signaling proteins like FAK, Shc, Grb2, Sos, Ras and Raf. Although the aforementioned results provide a clear link between increased NOS1 activity and myocardial hypertrophy, the fact that $NOS1^{-/-}$ mice develop cardiac hypertrophy and show increased premature mortality[50] indicates that NOS1 also plays a role in limiting myocardial hypertrophy. This suggests that the effects of NOS1-derived NO on cardiomyocyte size are context- and probably also dose-dependent.



### 4.4.2 Role of NOS2 in myocardial hypertrophy

NOS2 is absent in the healthy heart but its expression is induced by pro-inflammatory mediators as occurs during myocardial infarction and in heart failure,[51] and references herein]. In neonatal mouse cardiomyocyte cultures stimulated with 10 $\mu$g/mL LPS, *NOS2* expression was detectable from 6 h onwards.[11] In the present study induction of NOS2 by LPS treatment of NRCMs for 48 h resulted in an increase in CSA up to 40$\%$, dependent on the NOS2 level (fig. 7A). Although NOS2 was predominantly present in the cytosol, we noticed (sub)sarcolemmal accumulation of NOS2, especially at contact sites between NRCMs (fig. 7G) as has been described before.[33,52,53] Whether the localization of NOS2 immediately underneath the sarcolemma of NRCMs has any functional consequences remains to be investigated.

In a rat model of septic cardiomyopathy, induction of *NOS2* mRNA was detected as early as 30 min following injection of endotoxin (*i.e.* LPS), resulting in a peak of NOS2 activity after 6 h.[54] It is generally believed that inflammation-induced *NOS2* expression produces high levels of NO that may be toxic. Mice with myocardial *NOS2* overexpression suffered from cardiac fibrosis, myocardial hypertrophy (presumably of the pathological type) and ventricular dilatation, and displayed a high cardiomyocyte death rate.[55] Consistently, in $NOS2^{-/-}$ mice, aortic constriction caused less hypertrophy, dilatation, fibrosis and dysfunction of the left ventricle than in wild-type mice.[56] However, the idea that NOS2-derived NO is a major contributor to the development of heart failure has been challenged by Heger and colleagues, who did not observe any deleterious effects of myocardial NOS2 overexpression in hearts of transgenic mice.[57]

Role of NOS3 in myocardial hypertrophy Myocardial stretch leads to cardiomyocyte hypertrophy[49] and is believed to underlie the hypertrophic response of endurance exercise, aortic constriction and hypertension. Stretch-induced cardiomyocyte hypertrophy is coordinated by FAK/Src signaling,[58] in close connection with integrin stimulation.[6,7] In a recent study, Cheng and coworkers found that in NRCMs subjected to mechanical stretch *NOS3* expression and NOS3 activity are upregulated.[59] However, in the presence of L-

NAME, stretch-induced [$^3$H]-leucine incorporation into proteins was increased, whereas incubation of the cells with the NO donor S-nitroso-N-acetyl-DL-penicillamine inhibited stretch-induced protein synthesis. The authors hence concluded that NOS3 has a negative role in mechanical stretch-induced cardiomyocyte hypertrophy.[59] In keeping with the results of Cheng *et al.*, studies in *in vivo* models of myocardial infarction has led to the suggestion that cardiomyocyte-specific *NOS3* overexpression can limit compensatory hypertrophy in remote myocardium and preserve left ventricular performance.[60] Like *NOS1*$^{-/-}$ also *NOS3*$^{-/-}$ mice spontaneously develop cardiac hypertrophy, while combined *NOS1* and *NOS3* deficiency leads to even more pronounced myocardial hypertrophy.[50] On the basis of these results, Kempf and Wollert concluded that apparently the relatively low quantities of NO produced by the constitutive NOS isoforms under normal conditions protect from maladaptive (*i.e.* pathological) cardiac hypertrophy, such as induced by angiotensin-II, endothelin-1 and phenylephrine, which leads to adverse left ventricular remodeling and early death.

After having shown in this and previous studies[1,10] that signaling pathways downstream of stimulated integrins involve RyR2-associated NOS1, it is tempting to propose that this form of signaling leads to physiological hypertrophy. Evidence in favor of this view is the finding that (**i**) integrin stimulation-induced cardiomyocyte hypertrophy is associated with AKT phosphorylation (fig. 5A), (**ii**) AKT phosphorylation following treatment of NRCMs with an RGD motif-containing pentapeptide is reduced by L-NAME (fig. 5A) and (**iii**) wortmannin, an inhibitor of PI3K, inhibits dose-dependently the increase in NRCM surface area resulting from GRGDS-mediated integrin stimulation (fig. 5D). AKT is known to control phosphorylation of mTOR, S6K and glycogen synthase kinase-3$\beta$, three serine/threonine kinases involved in increased protein synthesis and cardiomyocyte hypertrophy.[61] AKT inhibition by SH-6, as well as transduction of NRCMs with a gene encoding a dominant-negative version of mouse AKT1, blocked GRGDS-induced NRCM hypertrophy which was associated with a decrease of phosphorylated S6K (fig. 6B). In addition, constitutive AKT signaling using iCA-AKT1 induced hypertrophy of NRCMs that was $\approx$50$\%$ inhibited by rapamycin, an inhibitor of mTOR which is a signaling protein downstream of AKT (fig. 6E).



### 4.4.3 Conclusion

The present study demonstrates that GRGDS-induced hypertrophy of NRCM is inhibited by (*i*) PIN, an endogenous inhibitor of NOS1, (*ii*) shRNA-mediated inhibition of *NOS1* expression and (*iii*) L-NAME, a general inhibitor of all NOS isoforms. However, this blockade can be rescued by administration of an exogenous NO donor, like SNP. In NRCMs, NO bioavailability thus is a regulator of GRGDS-induced hypertrophy and this regulatory pathway includes PI3K/AKT, suggesting that the process mimics physiological instead of pathological cardiac hypertrophy. Collectively, our results fit the model shown in fig. 8.

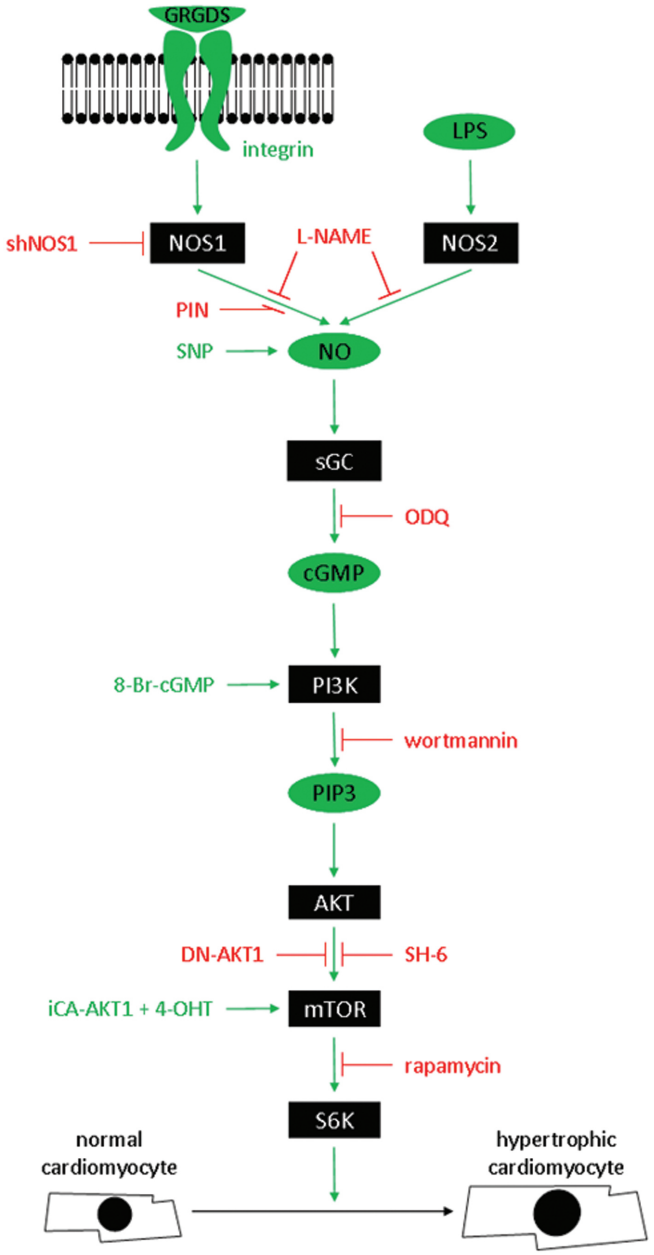


**Figure 4.8:** Model representation of the NO-dependent pathway leading to cardiomyocyte hypertrophy after integrin stimulation of NRCMs in culture. Only those factors that were directly or indirectly investigated in this study are indicated. Inhibitory and stimulatory interventions are indicated in red and green, respectively, and enzymes are indicated by black boxes.

## 4.5 Acknowledgements

The technical support from Minka Bax, Cindy Schutte, Lizet van der Valk and Margreet de Jong is gratefully acknowledged. We also thank Martine Moester for constructing the SIN-LV shuttle plasmid pLV.CMV.iCA-AKT1.IRES.eGFP.

## 4.6 References

1. Umar S, van der Valk EJM, Schalij MJ, van der Wall EE, Atsma DE, van der Laarse A. Integrin stimulation-induced hypertrophy in neonatal rat cardiomyocytes is NO-dependent. Mol Cell Biochem. 2009; 320:75-84.
2. Jaalouk DE, Lammerding J. Mechanotransduction gone awry. Nat Rev Mol Cell Biol. 2009; 10:63-73.
3. Ross RS, Borg TK. Integrins and the myocardium. Circ Res. 2001; 88:1112-1119.
4. Ingber DE. Cellular mechanotransduction: putting all the peices together again. FASEB J. 2006; 20:811-827.
5. Giancotti FG, Ruoslahti E. Integrin signaling. Science. 1999; 285:1028-1032.
6. Laser M, Willey CD, Jiang W, Cooper G IV, Menick DR, Zile MR, Kuppuswamy D. Integrin activation and focal complex formation in cardiac hypertrophy. J Biol Chem. 2000; 275:35624-35630. 7. Hynes RO. Integrins: bidirectional, allosteric signaling machines. Cell. 2002; 110:673-687.
8. Lal H, Verma SK, Foster DM, Golden HB, Reneau JC, Watson LE, Singh H, Dostal DE. Integrins and proximal signaling mechanisms in cardiovascular disease. Front Biosci. 2009; 14:2307-2334.
9. Cabodi S, Di Stefano P, Leal Mdel P, Tinnirello A, Bisaro B, Morello V, Damiano L, Aramu S, Repetto D, Tornillo G, Defilippi P. Integrins and signal transduction. Adv Exp Med Biol. 2010; 674:43-54.
10. van der Wees CGC, Bax WH, van der Valk EJM, van der Laarse A. Integrin stimulation induces calcium signaling in rat cardiomyocytes by a NO-dependent mechanism. Pflügers Arch - Eur J Physiol. 2006; 451:588-595. 11. Peng T, Lu X, Lei M, Feng Q. Endothelial nitric-oxide synthase enhances lipopolysaccharide-stimulated tumor necrosis factor-$\alpha$ expression via cAMP-mediated p38 MAPK pathway in cardiomyocytes. J Biol Chem. 2003; 278:8099-8105.
12. Jaffrey SR, Snyder SH. PIN: an associated protein inhibitor of neuronal nitric oxide synthase. Science. 1996; 274:774-777.
13. Hammond J, Balligand J-L. Nitric oxide synthase and cyclic GMP signaling in cardiac myocytes: From contractility to remodeling. J Mol Cell Cardiol. 2012; 52:330-40.
14. Zhao Y, Brandish PE, DiValentin M, Schelvis JPM, Babcock GT, Marletta MA. Inhibition of soluble guanylate cyclase by ODQ. Biochemistry. 2000; 39:10848-10854.
15. Iemitsu M, Miyauchi T, Maeda S, Sakai S, Kobayashi T, Fujii N, Miyazaki H, Matsuda M, Yamaguchi I. Physiological and pathological cardiac hypertrophy induce different molecular phenotypes in the rat. Am J Physiol Regul Integr Comp Physiol. 2001; 281:R2029-R2036.
16. Dorn GW II, Robbins J, Sugden PH. Phenotyping hypertrophy. Eschew obfuscation. Circ Res. 2003; 92:1171-1175.
17. Dorn GW II. The fuzzy logic of physiological cardiac hypertrophy. Hypertension. 2007; 49:962-970.
18. Kemi OJ, Ceci M, Wisloff U, Grimaldi S, Gallo P, Smith GL, Condorelli G, Ellingsen O. Activation or inactivation of cardiac Akt/mTOR signaling diverges physiological from pathological hypertrophy. J Cell Physiol. 2008; 214:316-321.
19. Bernardo BC, Weeks KL, Pretorius L, McMullen JR. Molecular distinction between

physiological and pathological cardiac hypertrophy: experimental findings and therapeutic strategies. Pharmacol Ther. 2010; 128:191-227.
20. Li L, Hessel M, van der Valk L, Bax M, van der Linden I, van der Laarse A. Partial and delayed release of troponin-I compared with the release of lactate dehydrogenase from necrotic cardiomyocytes. Pflügers Arch - Eur J Physiol. 2004; 448:146-152.
21. van Tuyn J, Pijnappels DA, de Vries AAF, de Vries I, van der Velde-van Dijke I, Knaän-Shanzer S, van der Laarse A, Schalij MJ, Atsma DE. Fibroblasts from human post-myocardial infarction scar acquire properties of cardiomyocytes after transduction with a recombinant myocardin gene. FASEB J. 2007; 21:3369-3379.
22. Kohn AD, Takeuchi F, Roth RA. Akt, a pleckstrin homology domain containing kinase, is activated primarily by phosphorylation. J Biol Chem. 1996; 271:21920-21926.
23. Zhou BP, Hu MC, Miller SA, Yu Z, Xia W, Lin SY, Hung MC. HER-2/neu blocks tumor necrosis factor-induced apoptosis via the Akt/NF-kappaB pathway. J Biol Chem. 2000; 275:8027-8031.
24. Shiojima I, Yefremashvili M, Luo Z, Kureishi Y, Takahashi A, Tao J, Rosenzweig A, Kahn CR, Abel ED, Walsh K. Akt signaling mediates postnatal heart growth in response to insulin and nutritional status. J Biol Chem. 2002; 277:37670-37677.
25. Friebe A, Koesling D. Regulation of nitric-oxide sensitive guanylate cyclase. Circ Res. 2003; 93:96-105.
26. Pyriochou A, Papapetropoulos A. Soluble guanylate cyclase: more secrets revealed. Cell Signal. 2005; 17:407-413.
27. Legate KR, Wickström SA, Fässler R. Genetic and cell biological analysis of integrin outside-in signaling. Genes Dev. 2009; 23:397-418.
28. Condorelli G, Drusco A, Stassi G, Bellacosa A, Roncarati R, Iaccarino G, Russo MA, Gu Y, Dalton N, Chung C, Latronico MVG, Napoli C, Sadoshima J, Croce CM, Ross J jr. Akt induces enhanced myocardial contractility and cell size *in vivo* in transgenic mice. Proc Natl Acad Sci - USA. 2002; 99:12333-12338.
29. Matsui T, Li L, Wu JC, Cook SA, Nagoshi T, Picard MH, Liao R, Rosenzweig A. Phenotypic spectrum caused by transgenic overexpression of activated Akt in the heart. J Biol Chem. 2002; 277:22896-22901.
30. Shioi T, McMullen JR, Kang PM, Douglas PS, Obata T, Franke TF, Cantley LC, Izumo S. Akt/protein kinase B promotes organ growth in transgenic mice. Mol Cell Biol. 2002; 22:2799-2809.
31. Pearson RB, Dennis PB, Han J-W, Williamson NA, Kozma SC, Wettenhall REH, Thomas G. The principal target of rapamycin-induced p70s6k inactivation is a novel phosphorylation site within a conserved hydrophobic domain. EMBO J. 1995; 14:5279-5287.
32. Xie Q-W, Kashiwabara Y, Nathan C. Role of transcription factor NK-$\kappa$B/Rel in induction of nitric oxide synthase. J Biol Chem. 1994; 269:4705-4708.
33. Buchwalow IB, Schulze W, Karczewski P, Kostic MM, Wallukat G, Morwinski R, Krause EG, Müller J, Paul M, Slezak J, Luft FC, Haller H. Inducible nitric oxide synthase in the myocard. Mol Cell Biochem. 2001; 217:73-82.
34. McCauley SD, Gilchrist M, Befus AD. Regulation and function of the protein inhibitor of nitric oxide synthase (PIN)/dynein light chain 8 (LC8) in a human mast cell line. Life Sci. 2007; 80:959-964.
35. Fan JS, Zhang Q, Li M, Tochio H, Yamazaki T, Shimizu M, Zhang M. Protein inhibitor

of neuronal nitric-oxide synthase, PIN, binds to a 17-amino acid residue fragment of the enzyme. J Biol Chem. 1998; 273:33472-33481.
36. Balija TM, Lowry SF. Lipopolysaccharide and sepsis-associated myocardial dysfunction. Curr Opin Infect Dis. 2011; 24:248-253.
37. Clemente CFMZ, Xavier-Neto J, Dalla Costa AP, Consonni SR, Antunes JE, Rocco SA, Pereira MB, Judice CC, Strauss B, Joazeiro PP, Matos-Souza JR, Franchini KG. Focal adhesion kinase governs cardiac concentric hypertrophic growth by activating the AKT and mTOR pathways. J Mol Cell Cardiol. 2012; 52:493-501.
38. Brenman JE, Xia H, Chao DS, Black SM, Bredt DS. Regulation of neuronal nitric oxide synthase through alternative transcripts. Dev Neurosci. 1997; 19:224-231.
39. Boissel J-P, Schwarz PM, Föstermann U. Neuronal-type NO synthase: transcript diversity and expeonential regulation. Nitric Oxide. 1998; 2:337-349.
40. Wang Y, Newton DC, Marsden PA. Neuronal NOS : Gene structure, mRNA diversity, and functional relevance. Crit Rev Neurobiol. 1999; 13:21-43.
41. Zhou L, Zhu D-Y. Neuronal nitric oxide synthase: Structure, subcellular localization, regulation, and clinical applications. Nitric Oxide. 2009; 20:223-230.
42. Barouch LA, Harrison RW, Skaf MW, Rosas GO, Cappola TP, Kobeissi ZA, Hobai IA, Lemmon CA, Burnett AL, O'Rourke B, Rodriguez ER, Huang PL, Lima JAC, Berkowitz DE, Hare JM. Nitric oxide regulates the heart by spatial confinement of nitric oxide synthase isoforms. Nature. 2002; 416:337-340.
43. Gonzalez DR, Beigi F, Treuer AV, Hare JM. Deficient ryanodine receptor S-nitrosylation increases sarcoplasmic reticulum calcium leak and arrhythmogenesis in cardiomyocytes. Proc Natl Acad Sci - USA. 2007; 104:20612-20617.
44. Ziolo MT, Kohr MJ, Wang H. Nitric oxide signaling and the regulation of myocardial function. J Mol Cell Cardiol. 2008; 45:625-632.
45. Loyer X, Vinet L, Wang Y, Milliez P, Robidel E, Jaisser F, Samuel J-L, Heymes C. Role of myocardial neuronal nitric oxide synthase in the development of cardiac hypertrophy. J Mol Cell Cardiol. 2006; 40:950 (abstract).
46. Loyer X, Gómez AM, Milliez P, Fernandez-Velasco M, Vangheluwe P, Vinet L, Charue D, Vaudin E, Zhang W, Sainte-Marie Y, Robidel E, Marty I, Mayer B, Jaisser F, Mercadier J-J, Richard S, Shah AM, Bénitah J-P, Samuel J-L, Heymes C. Cardiomyocyte overexpression of neuronal nitric oxide synthase delays transition toward heart failure in response to pressure overload by preserving calcium cycling. Circulation. 2008; 117:3187-3198.
47. McMullen JR, Shioi T, Huang WY, Zhang L, Tarnavski O, Bisping E, Schinke M, Kong S, Sherwood MC, Brown J, Riggi L, Kang PM, Izumo S. The insulin-like growth factor 1 receptor induces physiological heart growth via the phosphoinositide 3-kinase (p110alpha) pathway. J Biol Chem. 2004; 279:4782-4793.
48. Molkentin JD, Dorn GW 2nd. Cytoplasmic signaling pathways that regulate cardiac hypertrophy. Annu Rev Physiol. 2001; 63:391-426.
49. Ruwhof C, van der Laarse A. Review. Mechanical stress-induced cardiac hypertrophy: Mechanisms and signal transduction pathways. Cardiovasc Res. 2000; 47:23-37.
50. Kempf T, Wollert KC. Nitric oxide and the enigma of cardiac hypertrophy. BioEssays. 2004; 26:608-615. 51. Umar S, van der Laarse A. Nitric oxide and nitric oxide synthase isoforms in the normal, hypertrophic, and failing heart. Mol Cell Biochem 2010;333:191-

201. 52. Ringheim GE, Pan J. Particulate and soluble forms of the inducible nitric oxide synthase are distinguishable at the amino terminus in RAW 264.7 macrophage cells. Biochem Biophys Res Commun. 1995; 210:711-716.
53. Navarro-Lérida I, Corvi MM, Barrientos AA, Gavilanes F, Berthiaume LG, Rodríguez-Crespo I. Palmitoylation of inducible nitric-oxide synthase at Cys-3 is required for proper intracellular traffic and nitric oxide synthesis. J Biol Chem. 2004; 279:55682-55689.
54. Bateson AN, Jakiwczyk OM, Schulz R. Rapid increase in inducible nitric oxide synthase gene expression in the heart during endotoxemia. Eur J Pharmacol. 1996; 303:141-144.
55. Mungrue IN, Gros R, You X, Pirani A, Azad A, Csont T, Schulz R, Butany J, Stewart DJ, Husain M. Cardiomyocyte overexpression of iNOS in mice results in peroxynitrite generation, heart block, and sudden death. J Clin Invest. 2002; 109:735-743.
56. Zhang P, Xu X, Hu X, van Deel ED, Zhu G, Chen Y. Inducible nitric oxide synthase deficiency protects the heart from systolic overload-induced ventricular hypertrophy and congestive heart failure. Circ Res. 2007; 100:1089-1098.
57. Heger J, Gödecke A, Flögel U, Merx MW, Molojavyi A, Kühn-Velten WN, Schrader J. Cardiac-specific overexpression of inducible nitric oxide synthase does not result in severe cardiac dysfunction. Circ Res. 2002; 90:93-99. 58. Torsoni AS, Constancio SS, Nadruz W jr, Hanks SK, Franchini KG. Focal adhesion kinase is activated and mediates the early hypertrophic response to stretch in cardiac myocytes. Circ Res. 2003; 93:140-147.
59. Cheng T-H, Chen JJ-W, Shih N-L, Lin J-W, Liu J-C, Chen Y-L, Chen C-H, Chen J-J. Mechanical stretch induced endothelial nitric oxide synthase gene expression in neonatal rat cardiomyocytes. Clin Exp Pharmacol Physiol. 2009; 36:559-566.
60. Bloch KD, Janssens S. Cardiomyocyte-specific overexpression of nitric oxide synthase 3: Impact on left ventricular function and myocardial infarction. Trends Cardiovasc Med. 2005; 15:249-253.
61. Dorn GW 2nd, Force T. Protein kinase cascades in the regulation of cardiac hypertrophy. J Clin Invest. 2005; 115:527-537.